

# Studies on the corrosion behavior of lanthanum-implanted zircaloy\*

WAN QIAN<sup>‡</sup>

Department of Engineering Physics, Tsinghua University, Beijing 100084,  
People's Republic of China  
E-mail: wanqian99@tsinghua.org.cn

BAI XINDE

Department of Materials Science and Engineering, Tsinghua University, Beijing 100084,  
People's Republic of China

LIU XIAOYANG, ZHAO XIAO

Department of Engineering Physics, Tsinghua University, Beijing 100084,  
People's Republic of China

In order to study the effects of the lanthanum ion implantation on the aqueous corrosion behavior of zircaloy, specimens were implanted with lanthanum ions using a MEVVA source at an energy of 40 keV, with a dose range from  $5 \times 10^{16}$  to  $2 \times 10^{17}$  ions/cm<sup>2</sup> at about 150°C. The surface structure was investigated by X-ray Diffraction (XRD) and the valence of the lanthanum ions in the surface layer was analyzed by X-ray Photoemission Spectroscopy (XPS). Three-sweep potentiodynamic polarization measurement was employed to evaluate the aqueous corrosion behavior of zircaloy in a 0.5 M H<sub>2</sub>SO<sub>4</sub> solution. It was found that a significant improvement was achieved in the aqueous corrosion resistance of zircaloy compared with that of the as-received zircaloy. The mechanism of the corrosion resistance improvement of the lanthanum-implanted zircaloy is probably due to the addition of the lanthanum oxide dispersoid into the zircaloy matrix. © 2005 Springer Science + Business Media, Inc.

## 1. Introduction

Due to its low thermal neutron capture cross-section, good corrosion resistance, and adequate mechanical properties, zircaloy is often specified for engineering use in the nuclear industry. It is known that certain modification methods, such as ion beam surface processing (IBP), can significantly improve the corrosion resistance [1, 2]. Ion implantation, a kind of IBP, offers the possibility to introduce a controlled concentration of an element to a thin surface layer rapidly. It is first shown, by Ashworth *et al.*, that chromium implantation improved the corrosion resistance of iron [3]. Then, there is a growing interest in the application of ion implantation, as a valuable process for surface modification of materials. Many works including nitrogen implanted into titanium [4], molybdenum implanted into iron [5], and Tungsten implanted into aluminium [6] have proved that ion implantation can successfully improve the corrosion resistance without affecting the physical and mechanical stability of the bulk material.

Recently, the studies of yttrium ion implantation have devoted to the investigation of the corrosion

resistance of zircaloy [7–9]. However as the same group IIIA element to yttrium in the Chemical Periodic Table, little attention was paid concerning lanthanum ion implantation.

In this paper, the aqueous corrosion behavior of zircaloy implanted by lanthanum ions was studied, the surface structure characters of implanted layer was investigated by X-ray Diffraction (XRD), and the valence of the lanthanum ions was determined by X-ray photoemission spectroscopy (XPS). The mechanism of the aqueous corrosion resistance improvement of the lanthanum-implanted zircaloy was discussed.

## 2. Experimental details

The composition of zircaloy is presented in Table I. The specimens were cut from a sheet of zircaloy of 1.5 mm thickness and machined to 10 mm × 10 mm, mechanically polished with 200–1000 grade emery paper; then degreased in acetone and ethanol supersonically, chemically polished in the solution of 5 vol% HF, 45 vol% HNO<sub>3</sub>, 50 vol% H<sub>2</sub>O; and rinsed in the city water and de-ionized water subsequently.

\*Financed by Institute of Low Energy Nuclear Physics, Radiation Beam and Materials Laboratory, Beijing Normal University.

<sup>‡</sup>Author to whom all correspondence should be addressed.

TABLE I Composition of zircaloy (wt%)

Sn	Fe	Cr	Zr
1.4	0.23	0.1	bal

Zircaloy specimens were loaded onto a steel-made sample holder in the target chamber of the MEEVA implanter at a vacuum level of  $1 \times 10^{-4}$  Pa. The implanted area is of 12 cm diameter. The lanthanum implantation was carried out at an extracted voltage of 40 keV, and the beam current density was  $10 \mu\text{A}/\text{cm}^2$ . During implantation no special cooling was taken for the samples and the maximum temperature of the samples was  $150^\circ\text{C}$ . The implanted ions were at dose range from  $5 \times 10^{16}$  to  $2 \times 10^{17}$  ions/ $\text{cm}^2$ .

The surface structure character of the implanted layer was studied using a D/max XRD. The valence of the lanthanum ions in the surface layer was analyzed by a PHI5300 XPS.

In order to investigate the aqueous corrosion behavior of the lanthanum-implanted zircaloy, three-sweep potentiodynamic polarization measurements were carried out. Potentiodynamic tests were performed in a 0.5 M  $\text{H}_2\text{SO}_4$  solution using Zahner Elektrik IM6e potentiostat at room temperature ( $25^\circ\text{C}$ ). The working area was  $1 \text{ cm}^2$  and the scan rate was 2 mV/s. All electrochemical potential measurements were taken with respect to a saturated calomel electrode (SCE). The potentiodynamic polarization measurements were carried out as follows: an anodic scan was conducted starting in a cathodic region of approximately  $-0.5 \text{ V}$  with respect to the SCE and scanned into the anodic region of approximately  $+2.0 \text{ V}$  with respect to the SCE.

### 3. Results and discussions

#### 3.1. The surface structure of the lanthanum-implanted zircaloy

The surface structure of the lanthanum-implanted zircaloy specimens were examined by XRD. Fig. 1 shows the polycrystalline structure of the zircaloy im-

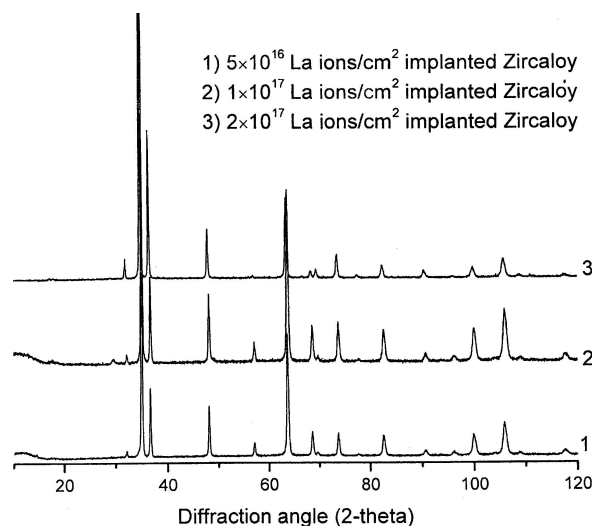


Figure 1 X-ray Diffraction (XRD) spectra of the Zircaloy specimens implanted with lanthanum ions at a dose range from  $5 \times 10^{16}$  to  $2 \times 10^{17}$  ions/ $\text{cm}^2$ .

planted by lanthanum ions at a dose range from  $5 \times 10^{16}$  to  $2 \times 10^{17}$  ions/ $\text{cm}^2$ . As shown in Fig. 1, it is clear that when the dose increased up to  $2 \times 10^{17}$  ions/ $\text{cm}^2$ , the structure is still polycrystalline and was not significantly changed under the lanthanum ion implantation. In some previous researches, it has been reported that the improvement of the corrosion resistance by ion implantation was attributed to the structure transformation from crystal to amorphous [10, 11]. However, this phenomenon does not happen in our experiment. The difference is due to the temperature of samples during implantation. In [10, 11], the samples were implanted at liquid nitrogen temperature. But the samples in our experiment were implanted at  $150^\circ\text{C}$ .

As we know, ion beam implantation always brings all kinds of defects to the surface of the materials, such as point defects and dislocation loops. The existence of these defects will change the matrix metal structure. If the implantation is conducted at liquid nitrogen temperature, most defects can be preserved. With the increase of defects, the structure can transform from crystal to amorphous. In our experiment, a large amount of defects, which formed during the lanthanum implantation, recovered at  $150^\circ\text{C}$ . Thus, the structure is still polycrystalline. Therefore, the improvement of properties by the lanthanum ion implantation is not attributed to structural changes in the zircaloy surface.

#### 3.2. The valence of the lanthanum ions in the surface layer

The valence of the lanthanum ions in the surface layer was analyzed by XPS. From the observation of the XPS spectra, the lanthanum ion is probably incorporated in the film as oxide. Fig. 2a and b are the experimental XPS spectra of C1s and La3d<sub>5/2</sub>, respectively. In Fig. 2a, the surface energy of the absorbed C on the surface of the specimen is 289.7 eV, which is 5.1 eV higher than the standard binding energy, 284.6 eV. The energy margin is due to the system error, and needs to be adjusted. The adjusted binding energy of the lanthanum ions is 834.3 eV, which coincides well with the standard values of  $\text{La}_2\text{O}_3$ , 834.9 eV, therefore, it can be said that the oxide of lanthanum in the surface exists in the form of  $\text{La}_2\text{O}_3$ .

#### 3.3. The electrochemical properties of the lanthanum-implanted zircaloy

It is found that there exists a great deal of oxygen in the surface layer of the lanthanum-implanted zircaloy using the XPS analysis. In order to study the electrochemical performance of a freshly exposed and oxide-free surface, the three-sweep potentiodynamic measurement was employed to eliminate the impact of thickened oxide film formed in air on the freshly implanted surface.

Fig. 3 summarizes the three-sweep potentiodynamic polarization curves of the as-received zircaloy in the 0.5 M  $\text{H}_2\text{SO}_4$  solution. It can be seen that the potentiodynamic polarization curve of the freshly exposed oxide-free surface is represented by the third sweep. This result was observed in previous works [10].

TABLE II Data of the corrosion potential  $E_{\text{corr}}$  (V vs. SCE) and implantation doses (ions/cm<sup>2</sup>)

Implantation dose	The first curve	The second curve	The third curve	The fourth curve	The mean value	Standard deviation
0	-0.2309	-0.2410	-0.2357	-0.2512	-0.2397	0.008706
$5 \times 10^{16}$	-0.05813	-0.05925	-0.05937	-0.06023	-0.05925	0.000862
$1 \times 10^{17}$	0.09075	0.08877	0.09123	0.09210	0.09071	0.00141
$2 \times 10^{17}$	0.1107	0.1153	0.1098	0.1210	0.1142	0.005134

TABLE III Data of the passive current density  $I_p$  (nA/cm<sup>2</sup>) and implantation doses (ions/cm<sup>2</sup>)

Implantation dose	The first curve	The second curve	The third curve	The fourth curve	The mean value	Standard deviation
0	58.28	57.37	56.25	59.88	57.95	1.534
$5 \times 10^{16}$	35.41	37.11	33.58	36.78	35.72	1.605
$1 \times 10^{17}$	23.51	25.33	20.48	21.56	22.72	2.145
$2 \times 10^{17}$	19.67	18.75	17.66	19.87	18.99	1.010

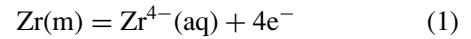
To reduce experiment error, four specimens were selected to perform potentiodynamic tests at each dose level. Three-sweep potentiodynamic polarization curves for each specimen were measured. The third curve was adopted to calculate the corrosion potential  $E_{\text{corr}}$  and the passive current density  $I_p$ . The measured data were listed in Tables II and III respectively.

According to the above table, the dependence of  $E_{\text{corr}}$  on the implanted dose and the relationship between  $I_p$  and the implanted doses are shown in Figs 4 and 5 respectively.

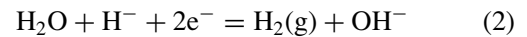
Comparing the corrosion behavior of the lanthanum-implanted zircaloy to that of the as-received zircaloy in Figs 4 and 5, it is clear that the corrosion potential,  $E_{\text{corr}}$  of the lanthanum-implanted zircaloy is much higher than that of the as-received zircaloy while the passive current density,  $I_p$  is much lower. It indicates that the aqueous corrosion resistance of zircaloy is significantly improved by the lanthanum ion implantation.

### 3.4. The mechanism of the improvement of the aqueous corrosion resistance by lanthanum ion implantation

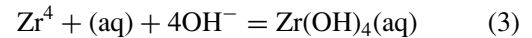
The formation of the passive film on surface of the zircaloy is an oxidation process. According to Pourbaix [12], there is an oxidation reaction that can take place at the zirconium anode:



The cathodic reactions may be:



when the anode supplies enough  $\text{Zr}^{4+}$  cations to the solution,  $\text{Zr}(\text{OH})_4$  immediately becomes saturated in solution as follows [13]:



According to above facts, the growth of the film is partially determined by the migration of zirconium ions.

It has been reported that the reactive elements, such as yttrium, cerium, and other rare earths, play an important role in the improvement of the corrosion properties [7, 14]. They always apply as a coating, or present as oxide dispersoid addition. In our case, the implanted lanthanum applies as oxide dispersoid addition. As analyzed above, after lanthanum ion implantation, the implanted lanthanum exists in the form of  $\text{La}_2\text{O}_3$  in the surface layer. The oxide dispersoid addition,  $\text{La}_2\text{O}_3$ , acts as a barrier to reduce the migration and dissolution of zirconium. So, the corrosion potential increases and the passive current density decreases. When the implantation dose increases, the density of the oxide dispersoid,  $\text{La}_2\text{O}_3$ , in the surface layer will increase, and the migration and dissolution of zirconium will be

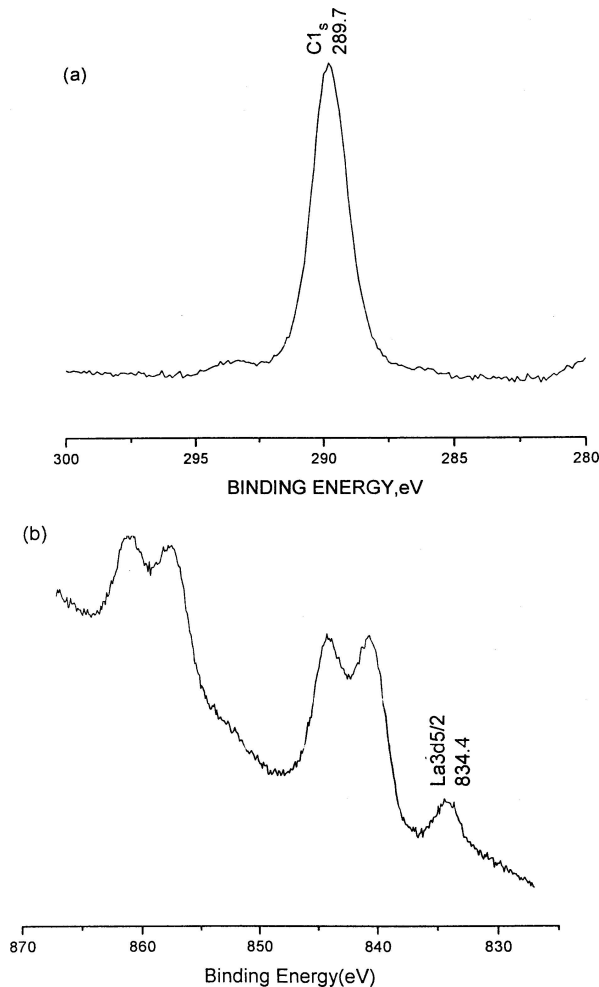


Figure 2 The X-ray Photoemission Spectroscopy (XPS) spectra of: (a) C1s peak and (b) La3d<sub>5/2</sub> peak in the implanted surface.

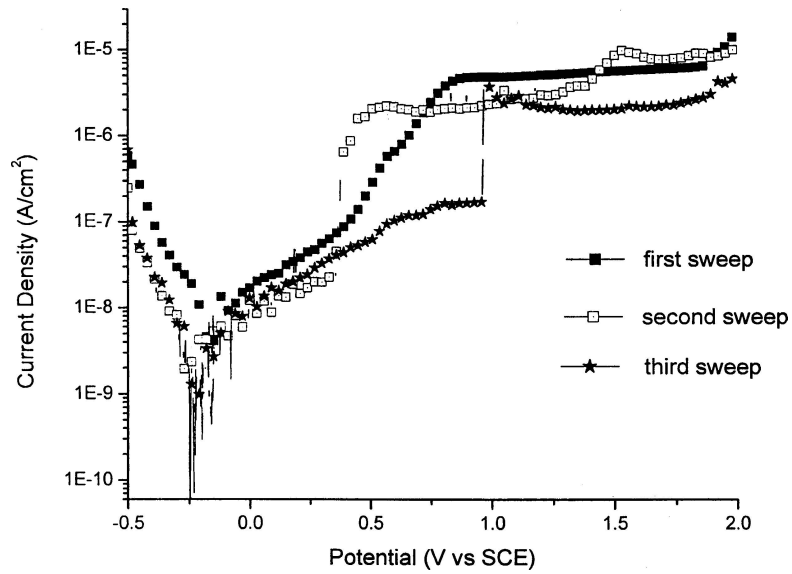


Figure 3 The three-sweep potentiodynamic polarization curves of the as-received zirconium in the 0.5 M H<sub>2</sub>SO<sub>4</sub> solution.

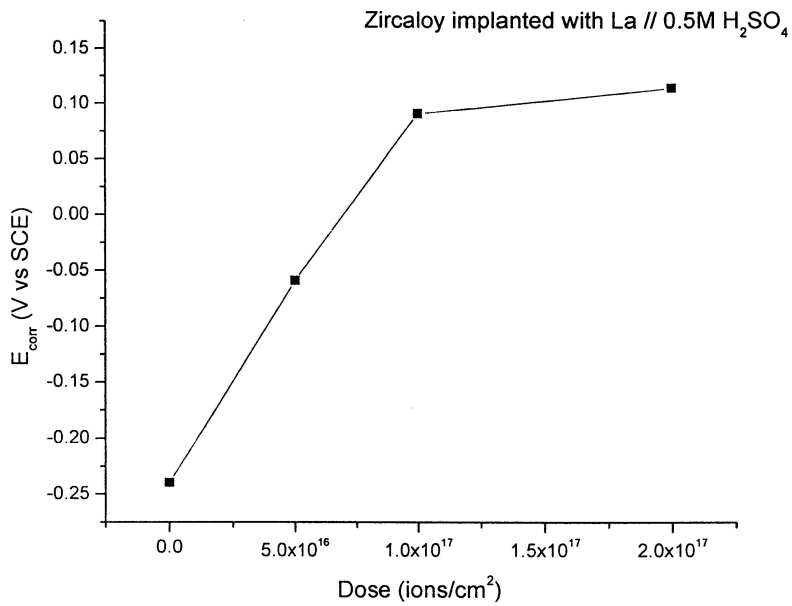


Figure 4 The dependence of the self corrosion potential vs. saturated calomel electrode (SCE).  $E_{\text{coit}}$ , on the implanted doses.

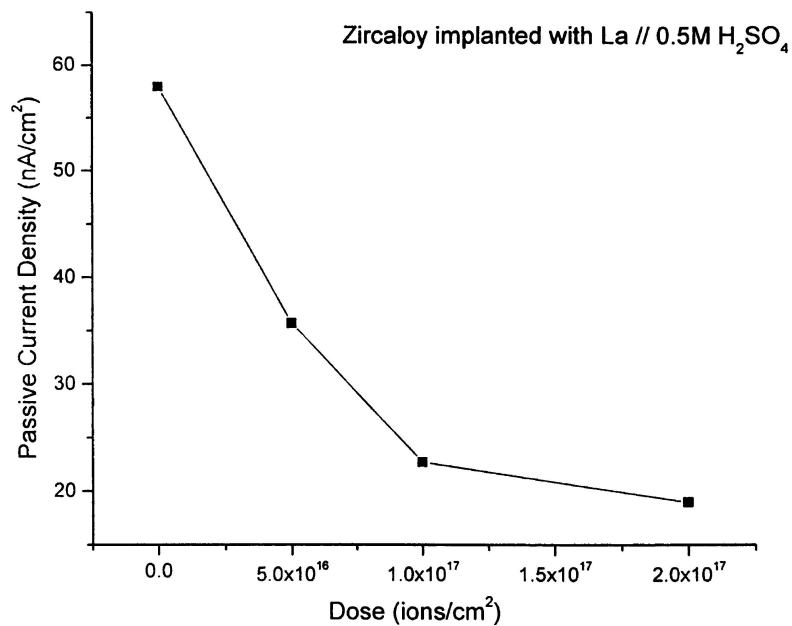


Figure 5 The dependence of passive current density  $I_p$  on the implantation doses.

more difficult, as a result, the potential  $E_{\text{corr}}$ , increases and the passive current density  $I_p$  decreases.

#### 4. Conclusions

(1) A significant improvement was achieved in the aqueous corrosion resistance of zircaloy by lanthanum ion implantation compared with that of the as-received zircaloy.

(2) The implanted lanthanum ions exist in the form of  $\text{La}_2\text{O}_3$  in the surface layer.

(3) The mechanism of the improvement of aqueous corrosion resistance is probably attributed to the addition of lanthanum oxide, but not to the structure transformation from polycrystalline to amorphous structure.

#### Acknowledgement

The authors wish to thank Engineer M. Chen for the kindness help in the lanthanum ions implantation.

#### References

1. J. JAGIELSKIJ, A. TUROS, G. GAWLIK *et al.*, *Nucl. Instrum Meth. B* **127** (1997) 961.

2. M. KLINGENBERG, J. ARPS and R. WEI, *Surf. Coat. Tech.* **158** (2002) 164.  
3. V. SHWORTH, D. BAXTER, W. A. GRANT *et al.*, *Corros. Sci.* **16** (1976) 775.  
4. M. YATSUZUKA, S. MIKI, R. MORITA *et al.*, *Vacuum*. **59** (2000) 330.  
5. D. WENG and M. WANG, *Mater. Chem. Phys.* **54** (1998) 338.  
6. C. M. RANGEL, M. A. TRAVASSOS and J. CHEVALLIER, *Surf. Coat. Tech.* **89** (1997) 101.  
7. J. XU, X. D. BAI, Y. D. FAN *et al.*, *J. Mater. Sci.* **35** (2000) 6225.  
8. J. XU, X. D. BAI, A. JIN *et al.*, *J. Mater. Sci. Lett.* **19** (2000) 1633.  
9. X. D. BAI, J. XU, F. HE *et al.*, *Nucl. Instrum. Meth. B* **160** (2000) 49.  
10. X. D. BAI, D. H. ZHU and B. X. LIU *ibid.* **103** (1995) 440.  
11. M. F. STROOSNIJDER, J. D. SUNDERKOTTER, M. J. CRISTOBAL *et al.*, *Surf. Coat. Tech.* **83** (1996) 205.  
12. M. POURBAIX, in "Atlas of Electrochemical Equilibria in Aqueous Solutions" (N.A.C.E., Houston, TX, 1974) p. 223.  
13. C. F. BAES and R. E. MESMER JR, in "The Hydrolysis of Cations" (Wiley, New York, 1976) p. 147.  
14. F. J. PEREZ, E. OTERO, M. P. HIERRO *et al.*, *Surf. Coat. Tech.* **109** (1998) 121.

Received 22 October 2002  
and accepted 29 April 2004